

Rigorous Hybrid Field Theoretic Design of Stepped Rectangular Waveguide Mode Converters Including the Horn Transitions into Half-Space

THOMAS WRIEDT, KARL-HEINZ WOLFF, FRITZ ARNDT, SENIOR MEMBER, IEEE, AND ULRICH TUCHOLKE

Abstract—A full-wave hybrid field theoretic method is presented for the accurate and efficient computer-aided design of complete microwave or millimeter-wave radiating components comprising stepped rectangular waveguide mode converters and horn transitions including the effect of the aperture radiating into halfspace. The hybrid method combines the complete six-field component modal S-matrix formulation, for the double-plane waveguide discontinuity problem of the throat section, with the full component moment solution, for the aperture problem. Two orthogonally polarized sets of rooftop basis functions are utilized to model the magnetic surface currents in the apertures. All important design parameters, such as the input reflection coefficient including the actual aperture effect, H- and E-plane patterns considering the influence due to all excited higher order mode field components, as well as the cross-polarization characteristics, are rigorously taken into account by the design theory. The method is verified by comparison with available measured data for pyramidal horn transitions. Two design examples for stepped multimode horn transitions are presented. One example has been optimized with regard to pattern symmetry and achieves nearly identical E- and H-plane patterns from 10.8 to 11.2 GHz within $\Theta \in (-30^\circ, +30^\circ)$. The second example with optimized cross-polarization behavior shows -50 dB maximum cross-polarization level at 11 GHz.

I. INTRODUCTION

WAVEGUIDE APERTURES radiating into a half-space are an essential part of many microwave- and millimeter-wave components for various fields of application, such as material measurements, biomedical engineering, aeronautics antennas, and array feed elements, [1]–[34], [39], [52]. As improved properties, like symmetry of the *E*- and *H*-plane patterns and low sidelobe and cross-polarization levels, are desired for many purposes, the construction of appropriate mode converters and transitions between feeding waveguide and the aperture has been the subject of many papers, e.g. [14]–[34], [39]. Although most of the research work was hitherto devoted to structures with circular cross section ([1]–[3], [6], [14]–[19], [22]–[24]), rectangular radiators are of growing interest [4], [9]–[13], [20], [21], [25]–[34], [39] [51]. This may be due to several advantages inherent to the Cartesian aperture format: flexibility in generating a wide variety of desired beam characteristics by suitably chosen aperture width or height, availability of relatively easy fabrication techniques, and many possibilities for simple integration of other common microwave components, such as

filters, polarizers, orthomode junctions, couplers etc. [35]–[39].

Many refined techniques for designing rectangular horn structures are available, based on impedance wall [17]–[21], diffraction [27], moment method, [29], [52], or simplified mode-matching solutions [28], [32]. However, increasing activity at millimeter-wave frequencies and the growing integration complexity of components may encourage interest in more accurate field theoretic methods which allow the efficient computer-aided design of the entire radiating system, taking into account both the complete set of higher order modes excited at the discontinuities in the throat section, and the actual aperture effect. Moreover, the well-known principle of dual mode horn transitions with stepped waveguide mode converters [14]–[16], [18], [26], [39], has turned out to be an attractive alternative to the well-established superior but more complicated, corrugated horn [17]–[19], [25], [28], [30]–[32], for all cases where a simple, compact, low-cost, low-weight radiating element is required with good electrical properties within a limited relative bandwidth. This may be valid especially at short wavelengths, where corrugated horns are difficult to fabricate, and where the absolute operation frequency band may be sufficiently large for many applications [15]. The purpose of this paper, therefore, is to achieve an accurate field theoretic method for the computer-aided design of stepped rectangular waveguide mode converters and horn transitions into half-space (Fig. 1), which may be optimized with regard to all relevant parameters, such as the input voltage standing-wave ratio (VSWR) including the actual aperture effect, the *H*- and *E*-plane patterns considering the influence of all excited higher order modes as well as of their mutual interaction, and the cross-polarization characteristics.

Although more general ways to solve the stepped rectangular horn problem have been proposed more recently [28], [29], [32], [49], [50], there still exist some essential restrictions for the efficient computer-aided design of such components. In [28], [30], the reflection and mode conversion effects at the aperture discontinuity are not taken into account (or only approximately considered by a fictitious cavity module [30]). This influence has turned out to be important [32], [51], also for apertures exceeding the dimension of about three wavelengths [28], [30]. The TE_{mn}^x -wave formulation used in [13], [32], [49], [50], neglects important higher order modes and field components, excited at a typical double-plane step discontinuity [35], or at rectangular apertures, as well as

Manuscript received November 19, 1987.

The authors are with the Microwave Department, University of Bremen, Kufsteiner Str. NW1, D-2800 Bremen 33, West Germany.

IEEE Log Number 8927253.

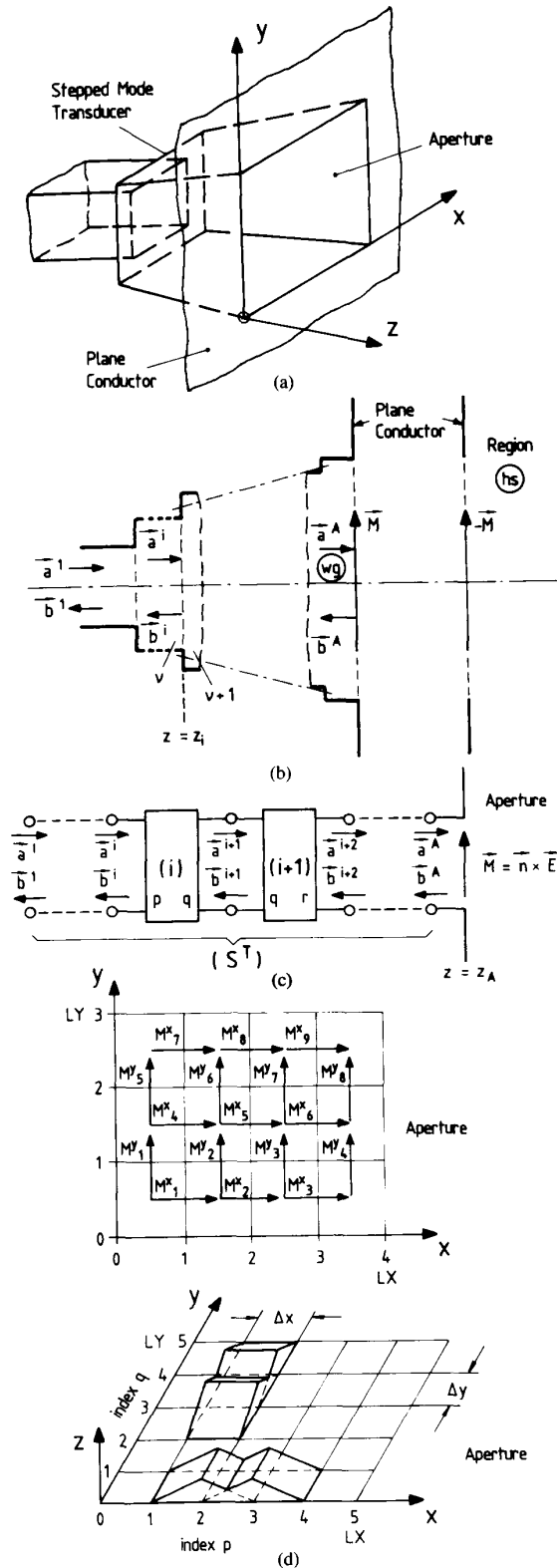


Fig. 1. Modeling of the mode converter, horn transition, and the aperture. (a) Stepped mode transducer and horn transition. (b) Stepped waveguide section and equivalence principle. (c) Modal scattering matrix of the throat region. (d) Orthogonally polarized sets of rooftop expansion functions for the magnetic surface current.

relevant coupling effects between them. Therefore this method fails to predict important pattern characteristics, such as the cross-polarization behavior.

The full-wave hybrid field theory method presented in this paper solves the entire stepped rectangular horn problem without the usual restrictions. The double-plane waveguide step discontinuities (Figs. 1(a), 1(b)) are treated by utilizing the rigorous six-field component formulation given in [35], and the aperture problem is attacked by the moment method [5], proven for this kind of problem, by using two orthogonally polarized sets of rooftop basis functions (Figs. 1(b), 1(c)) to model the magnetic surface currents in the aperture. The immediate modal-S-matrix combination utilized, for all interacting structures, preserves numerical accuracy, since the expressions contain exponential functions with only negative argument. This procedure avoids numerical instabilities caused by the otherwise known situation of interacting discontinuities if evanescent modes are involved. A further advantage is that no symmetry of ports or modes is required. Therefore, e.g., there is no need to maintain the number of “localized” modes [40], necessary for modeling the step discontinuities, for the “accessible” modes [40], between them. Moreover, multiport components, such as *E*- or *H*-plane septa for beam equalizing [41], may be included in the theory. For computer optimization, the evolution strategy method [42], i.e., a suitably modified direct search procedure, is applied where no differentiation step in the optimization process is necessary, and hence the problem of local minima may be circumvented. The theory is verified by available measured data for pyramidal horns. The efficiency of the computer-aided design program is demonstrated via a design example for an optimized stepped multimode horn at 11 GHz.

II. THEORY AND DESIGN

A. Stepped Rectangular Waveguide Throat Section

For the calculation of the stepped waveguide section (cf. Figs. 1(a) and 1(b)), comprising the stepped mode converter and the horn transition (simulated by means of a staircase function with a sufficient number of steps), the modal-S-matrix method is applied [35]–[38], [43], which has already proved to be highly appropriate for the accurate design of many waveguide components. Similar to the field theory treatment of filters [35], couplers [37], or transformers [43], the throat structure is decomposed into appropriate key building blocks (homogeneous waveguide sections, and the double-plane step discontinuity [35]). The modal scattering matrix of the total throat section (Figs. 1(b), 1(c))

$$\begin{pmatrix} \vec{b}^1 \\ \vec{a}^A \end{pmatrix} = (S^T) \begin{pmatrix} \vec{a}^1 \\ \vec{b}^A \end{pmatrix}, \quad (1)$$

is calculated by suitable direct combination of the single modal scattering matrices (*S*)⁽ⁱ⁾, (*S*)⁽ⁱ⁺¹⁾ (cf. Fig. 1(c))

$$\begin{pmatrix} \vec{b}^i \\ \vec{a}^{i+2} \end{pmatrix} = (S^{\text{comb}}) \begin{pmatrix} \vec{a}^i \\ \vec{b}^{i+2} \end{pmatrix}, \quad (2)$$

by an iteration formulation [35], [43], given in the Appendix using the present notation. This procedure helps to maintain

numerical stability and provides high flexibility concerning mode or port numbers in the single iteration steps, since no symmetry of ports is required as is indicated in Fig. 1(c) by p , q , r , respectively.

The derivation of the required key building block modal- S -matrix of a double-plane step module ν (Figs. 1(b), (c)) is well known [35], [43]; the theory is given here in abbreviated form only. The complete modal field in the related subregions i ($= \nu, \nu + 1$) of the module ν (Fig. 1(b))

$$\vec{E}^{(i)} = -j\omega\mu\nabla \times \vec{\Pi}_{hz}^{(i)} + \nabla \times \nabla \times \vec{\Pi}_{ez}^{(i)} \quad (3a)$$

$$\vec{H}^{(i)} = j\omega\epsilon\nabla \times \vec{\Pi}_{ez}^{(i)} + \nabla \times \nabla \times \vec{\Pi}_{hz}^{(i)} \quad (3b)$$

is derived from the axial components of the magnetic and electric Hertzian vector potentials $\vec{\Pi}_h$ and $\vec{\Pi}_e$, respectively, which are represented as the sum of the complete set of eigenmodes [35], [43]

$$\begin{aligned} \Pi_{hz}^{(i)} = & \sum_{m=0}^M \sum_{n=0}^N [a_{hmn}^{(i)} \cdot \exp(-\gamma_{hmn}^{(i)}z) \\ & + b_{hmn}^{(i)} \cdot \exp(+\gamma_{hmn}^{(i)}z)] \cdot T_{hmn}^{(i)} \cdot \frac{-j}{\omega\epsilon} \cdot \sqrt{Z_{hmn}^*} \end{aligned} \quad (4a)$$

$$\begin{aligned} \Pi_{ez}^{(i)} = & \sum_{m=1}^M \sum_{n=1}^N [a_{emn}^{(i)} \cdot \exp(-\gamma_{emn}^{(i)}z) \\ & - b_{emn}^{(i)} \cdot \exp(+\gamma_{emn}^{(i)}z)] \cdot T_{emn}^{(i)} \cdot \frac{-j}{\omega\mu} \cdot \sqrt{Y_{emn}}. \end{aligned} \quad (4b)$$

By utilizing the usual field matching relations, [3], [35], [43], at the corresponding interface $z = z_i$, (Fig. 1(b)), the still unknown wave amplitude coefficients in the forward and backward direction, \mathbf{a} and \mathbf{b} , respectively, are related to each other in order to obtain the modal scattering matrix (S)⁽ⁱ⁾ directly. The cross-section eigenfunctions \mathbf{T} are suitably normalized [35], [43]. As the knowledge of these is required also for formulating the normalized wave amplitude coefficients in the solution of the aperture problem, the explicit expressions for \mathbf{T} are given in the Appendix using the present notation. γ_h , γ_e are the propagation constants, and Z_h , or Y_e , are the wave impedances, or admittances, of the m th TE, and TM mode, respectively, under consideration. The asterisk denotes the conjugate complex value which is due to the normalization to the complex power.

All TE _{mn} and TM _{mn} modes are required for solving accurately the general double-plane step discontinuity problem. For concentric axes, the related mode numbers in the summations of (4) are $m = 1, 3, 5, \dots$, and $n = (0), 2, 4, \dots$. Note further that TE waves are coupled with the TM waves; this effect is rigorously taken into account by (1)–(4). Due to the technique of direct combination of the single scattering matrices, it has turned out that modes up to the order $M = 5$ and $N = 4$, i.e., TM₅₄ and TE₅₄, are all that are required in the calculations for the designs given in this paper to yield sufficient asymptotic behavior of the scattering coefficients. The final data have been checked by an expansion up to TM₉₈, TE₉₈. For calculating the continuously tapered

horn sections, a step-model with about 60 waveguide double-plane steps is used which provides sufficient asymptotic behavior, as has been checked by considering more than 100 steps. An adequate phase term [18] for each mode considered is added to account for the curvature of the wavefront.

B. The Aperture Problem

The aperture discontinuity problem (Fig. 1(b)) is advantageously solved with the moment method [5], by using two orthogonally polarized rooftop expansion functions for the magnetic surface currents in the apertures. Therefore, large aperture sizes, the influence of higher order modes, and the cross-polarization effects, are taken into account, accurately. Moreover, multiple apertures may be included in the theory by simply extending the corresponding relations by an appropriate summation over the related apertures. As the moment method is already well-established, [5], [7], [8], [10], [44]–[48], the general part of the theory is presented in abbreviated form only.

The aperture discontinuity (Fig. 1(b)) is divided into two separate regions through the use of the equivalence principle, [3], [5], [7], [8], [10]. The equivalent magnetic surface currents $+\vec{M}$ and $-\vec{M}$, placed on the waveguide and half-space side of the aperture plane are related to the electric field \vec{E} in the aperture by

$$\vec{M} = \vec{n} \times \vec{E}, \quad (5)$$

where \vec{n} is the unit vector normal to the aperture. Continuity of the tangential magnetic field \vec{H}_{tan} across the aperture is expressed in its usual form [5], [7], [8], [10]

$$\vec{H}_{\text{tan}}^{\text{wg}}(\vec{M}) - \vec{H}_{\text{tan}}^{\text{hs}}(-\vec{M}) = -\vec{H}_{\text{tan}}^{\text{inc}}; \quad (6)$$

“wg” and “hs” denote the waveguide side and the half-space side of the aperture plane, respectively; “inc” denotes the incident field.

As large waveguide elements and higher order modes are included in the theory, two orthogonally polarized sets of overlapping rooftop basis functions \vec{M}^x and \vec{M}^y (Figs. 1(d), (e)) are used to model the magnetic surface currents in the aperture. The aperture is subdivided into LX , and LY segments in the x and y directions, respectively, resulting in patches of size $\Delta x \cdot \Delta y$. The basis function expansion may be written in the abbreviated form [17],

$$\vec{M} = \sum_{l=1}^{NE} V_l \cdot \vec{M}_l, \quad (7)$$

with the total number NE of expansion functions $NE = (LX - 1)LY + (LY - 1)LX$, and where V_l is a complex coefficient to be determined. \vec{M}^x and \vec{M}^y are given by (cf. Figs. 1(d), (e))

$$\begin{aligned} \vec{M}_{pq_x}^x &= \vec{n}_x Q_{p_x}^x(x) \cdot P_{q_x}^y(y) \\ \vec{M}_{pq_y}^y &= \vec{n}_y Q_{p_y}^y(y) \cdot P_{q_y}^x(x) \end{aligned} \quad (8)$$

where \vec{n}_x , \vec{n}_y are unit vectors in the x -, and y -directions, and Q and P are triangular and pulse functions [46], [8], respectively. The abbreviations in (8) are elucidated in the Appendix.

Substituting (7) in (6) yields the matrix equation in the well-known abbreviated form [7],

$$[(Y^{\text{wg}}) + (Y^{\text{hs}})] \cdot \vec{V} = \vec{I}^{\text{inc}} \quad (9)$$

with generalized elements (Y), \vec{V} , \vec{I}^{inc} , due to the inclusion of NE orthogonally polarized surface current expansion functions, and with MN TE and TM modes considered in the waveguide.

The admittance matrix (Y^{hs}) of the half-space region of size $NE \times NE$, including the orthogonally polarized expansion \vec{M}_t and weighting functions \vec{W}_s according to (7) and Galerkin's method, is calculated analogously to [5], [7], [8], [10], [44]–[48]

$$Y_{st}^{\text{hs}} = - \iint_{\text{aperture}} (\vec{n}_x W_s^x + \vec{n}_y W_s^y) \cdot \vec{H}_{\text{tan}}^n(\vec{M}_t^x, \vec{M}_t^y) \cdot da, \quad (10)$$

where \vec{H}_{tan}^n (cf. Appendix) is the normalized tangential magnetic field in the aperture due to all TE and TM modes considered.

The waveguide admittance matrix (Y^{wg}) of size $NE \times NE$ is formulated by using the summation over the complete set of TE and TM modes included in the throat region

$$Y_{st}^{\text{wg}} = \sum_{k=0}^M \sum_{l=0}^N A_{thkl}^{\text{wg}} \cdot B_{shkl}^{\text{wg}} + \sum_{k=1}^M \sum_{l=1}^N A_{tekl}^{\text{wg}} \cdot B_{sekl}^{\text{wg}} \quad (11)$$

with the coefficients \mathbf{A} , \mathbf{B} , which are formulated by the inner product containing the expansion and weighting functions, respectively, the normalized field amplitudes as well as the wave admittances of all TE and TM modes considered (cf. Appendix).

The current excitation vector in (9) is given by

$$\begin{aligned} \vec{I}_s^{\text{inc}} = & 2j\sqrt{Y_{hkl}^*} \cdot [(U) - S_{22hkl}^T \cdot S_{11}^A]^{-1} \cdot S_{21hkl}^T \\ & \cdot B_{shkl}^{\text{wg}} \cdot a_{hkl}^1 + 2(-j\sqrt{Y_{ekl}}) \cdot [(U) - S_{22ekl}^T \\ & \cdot S_{11}^A]^{-1} \cdot S_{21ekl}^T \cdot B_{sekl}^{\text{wg}} \cdot a_{ekl}^1 \end{aligned} \quad (12)$$

where \mathbf{Y} , \mathbf{B} are explained in the Appendix (25), (23); \mathbf{a}^1 is the vector of the wave amplitudes incident at port 1 (Figs. 1(b), (c)), (S^T) is the overall modal scattering matrix (1) of the throat region, (U) is the unit matrix, and S_{11}^A is the submatrix of the reflection coefficients at the aperture, cf. (14).

A computer program was written using the preceding equations. Equation (9) is solved by the known method of moments. The antenna characteristics are calculated using the usual relations. The input reflection matrix (S_{11}) at port 1 of the feeding waveguide including the aperture discontinuity effect is given by

$$(S_{11}) = [(S_{11}^T) + (S_{12}^T)(S_{11}^A)] \cdot [(U) - (S_{22}^T)(S_{11}^A)]^{-1} \cdot (S_{21}^T). \quad (13)$$

The submatrix (S_{11}^A) of the reflection coefficients at the aperture is calculated by the relation of the reflected to the incident mode amplitudes, which may be formulated accord-

ing to [49] by

$$(S_{11}^A) = [(Y^{\text{wg}}) + (Y^{\text{hs}})]^{-1} \cdot [(Y^{\text{wg}}) - (Y^{\text{hs}})]. \quad (14)$$

The cross-polarization investigation is based on Ludwig's third definition [18]. For the numerical examples presented in this paper, the rectangular apertures have been subdivided into $LX = 4$ segments in the x -direction and $LY = 3$ segments in the y -direction. This achieves sufficient asymptotic behavior of the corresponding radiation and reflection characteristics as has been checked by a subdivision up to seven elements.

C. Design

As with single components, such as transformers [43], polarizers [36], and couplers [37], [38], the computer-aided design of the complete radiating assembly, which is composed of the rectangular waveguide mode converter, the horn transition, and the aperture discontinuity (Figs. 1(a), 1(b), 1(c)), is carried out by an optimizing program applying the evolution strategy method [42]. An error function [36]–[38], [42], [43], may be defined comprising the desired parameters to be minimized: symmetry of the E - and H -plane pattern within a desired scan angle range, maximum cross-polarization level, maximum sidelobe level, and maximum input reflection coefficient within a given frequency range.

In order to reduce the computing time required for the optimization of specific radiator types, however, it may be advantageous to utilize appropriate phase and magnitude relations for the modal scattering parameters in the throat region, which have turned out to be important for the overall design. For example, for a multimode horn designed for optimum pattern symmetry, in this paper, an error function

$$\begin{aligned} F(\vec{x}) = & \sum_{v=1}^V \left\{ \text{arc} \left[S_{21}^T \begin{matrix} \text{TE}_{10} \\ \text{TM}_{12} \end{matrix} (\vec{x}, f_v) \right] \right. \\ & - \text{arc} \left[S_{21}^T \begin{matrix} \text{TE}_{10} \\ \text{TE}_{10} \end{matrix} (\vec{x}, f_v) \right] - \pi \left. \right\}^2 / 3 \\ & + \left\{ \text{arc} \left[S_{21}^T \begin{matrix} \text{TE}_{10} \\ \text{TM}_{12} \end{matrix} (\vec{x}, f_v) \right] \right. \\ & - \text{arc} \left[S_{21}^T \begin{matrix} \text{TE}_{10} \\ \text{TE}_{12} \end{matrix} (\vec{x}, f_v) \right] \left. \right\}^2 / 3 \\ & + \left\{ \left| S_{21}^T \begin{matrix} \text{TE}_{10} \\ \text{TM}_{12} \end{matrix} (\vec{x}, f_v) \right| - 0.37 \right\}^2 \\ & + \left\{ \left| S_{21}^T \begin{matrix} \text{TE}_{10} \\ \text{TE}_{12} \end{matrix} (\vec{x}, f_v) \right| - 0.2 \right\}^2 + |S_{11}(\vec{x}, f_v)|^2 \end{aligned} \quad (15)$$

(where arc denotes the phase angle in radians), is minimized with respect to the parameter vector (\vec{x}) = (a_i, b_i, l_i)'. Here, f_v are the frequency sample points within the desired passband, and S_{21}^T, S_{11} are the calculated modal scattering parameters of the throat region and the overall component, respectively. The number V of frequency sample points was chosen to be equal to 20. For given feeding waveguide and aperture dimensions, and number of stepped mode transducer and horn sections, the

parameters \bar{x} to be optimized are the waveguide cross-section dimensions a_i , b_i , and the length l_i , of the i th transducer or horn section.

The advantages of the applied evolution strategy method [42], i.e., a suitably modified direct search procedure, are such that no differentiation step in the optimization process is necessary and hence the problem of local minima may be circumvented. A main optimization strategy parameter H , a secondary strategy parameter G , and a standard random variable $r \in (-1, +1)$ influence the alteration of the parameter vector (\bar{x}) during the optimization process with the standard deviation $\sigma = H \cdot G$ [42]. The new parameters $(\bar{x})_{\text{new}}$ are calculated at each iteration step by

$$(\bar{x})_{\text{new}} = (\bar{x})_{\text{old}} - r \cdot (\bar{x})_{\text{old}} \cdot \sigma \quad (16)$$

where $(\bar{x})_{\text{old}}$ are the preceding parameters. Initial values for H and G are chosen to be $H = 0.01$, $G = 1$. G may be utilized to modify the variation of the individual parameters. After a successful trial, H is doubled; for more than three unsuccessful trials, H is halved. If the error function is minimized three times by less than 0.2 percent, the result is interpreted as a local minimum. H is then multiplied by 10^4 . Thus, the optimization process begins again for a different parameter range. Note that in order to maintain physically realistic parameters, an appropriate variable transformation [42] is utilized.

III. RESULTS

Fig. 2(a) shows the relative field E -plane and H -plane patterns of a "standard-gain" pyramidal horn. The theoretically predicted patterns agree well with the measured values. The measured and predicted maximum cross-polarization level was -37 dB. In Fig. 2(b), for a pyramidal horn example with large flare angle, the relative field patterns calculated with the theory presented in this paper are plotted with the data available from [49]. As the theory of [13], [32], [49], [50] only considers the TE_{mn}^x field components, i.e., about one quarter of the complete set of modes excited in the throat, there are deviations between the results of [50] and our results of the order of some decibels. However, for the E -plane sectoral horn in Fig. 2(c), where a TE_{10} -wave incident on port 1 excites only longitudinal section TE_{mn}^x -waves at the discontinuities in the y -direction, i.e., where the TE_{mn}^x -modes represent the complete set of modes, good agreement between the results available from [50] and ours can be observed. For the input reflection coefficient of a pyramidal horn (Fig. 2(b)), there are only insignificant deviations between the theoretical results of [32] and ours. This is due to the fact that, for the reflection coefficient of rectangular waveguide discontinuities, for an incident TE_{10} -wave, the influence of the electric field component E_x (which is neglected in the TE_{mn}^x -formulation) is not dominant, cf. also [43].

As introduced by [14], the lack of axial pattern symmetry of standard horn transitions into half-space may be overcome by introducing the TE_{12} - and TM_{12} -modes along with the dominant TE_{10} -mode. The generation of these modes by a simple stepped mode transducer and by a rectangular horn transition with abruptly changing flare angle is illustrated in Fig. 3.

The efficiency of the computer-aided design program is demonstrated via two examples of optimized stepped multimode horn transitions. The first design example, which leads to a configuration as shown in Fig. 4(a), has been optimized using the error function (15) with regard to pattern symmetry. Nearly identical E - and H -plane patterns (Figs. 4(b)) are achieved within $\Theta \in (-30^\circ, +30^\circ)$. The bandwidth is about 10.8 – 11.2 GHz. Fig. 4(b) is shown for the more critical upper frequency limit. Fig. 4(c) presents the related modal scattering coefficients as a function of frequency.

As the maximum cross-polarization level (-22 dB) of the horn in Fig. 4(a) may be judged to be relatively high for many applications, a second design example has been optimized by utilizing the criterion of minimum cross polarization, directly, while the optimized horn configuration is shown in Fig. 5(a). The pattern symmetry (Fig. 5(b)) is less than for the first example, the cross-polarization behavior (Fig. 5(c)), is considered to be good.

IV. CONCLUSION

A computer-aided design method for complete rectangular waveguide radiating components is described which comprises multimode stepped mode converters, horn transitions and the aperture radiating into half-space. The full-wave hybrid field theoretic technique used permits the inclusion of all important parameters, such as the input reflection coefficient, taking the actual aperture effect into account, as well as the E - and H -plane pattern and the cross-polarization characteristics, by considering the influence due to all excited higher order mode field components. Application of a modified direct search method leads to optimized radiating characteristics and minimized cross-polarization levels, as has been demonstrated for relatively compact multimode horns designed for about 11 GHz. As the hybrid method combines the complete six-field component modal- S -matrix formulation of the throat section, with a complete moment solution for the aperture problem including two orthogonally polarized sets of basis functions, the theory agrees well with the measurements.

APPENDIX

A. Submatrices in (2)

$$\begin{aligned} S_{11}^{\text{comb}} &= S_{11}^{(i)} + S_{12}^{(i)} W_1 S_{11}^{(i+1)} S_{21}^{(i)} \\ S_{12}^{\text{comb}} &= S_{12}^{(i)} W_1 S_{12}^{(i+1)} \\ S_{21}^{\text{comb}} &= S_{21}^{(i+1)} W_2 S_{21}^{(i)} \\ S_{22}^{\text{comb}} &= S_{22}^{(i+1)} + S_{21}^{(i+1)} W_2 S_{22}^{(i)} S_{12}^{(i+1)} \end{aligned} \quad (17)$$

with

$$W_1 = [U - S_{11}^{(i+1)} S_{22}^{(i)}]^{-1}$$

$$W_2 = [U - S_{22}^{(i)} S_{11}^{(i+1)}]^{-1}$$

U = unit matrix.

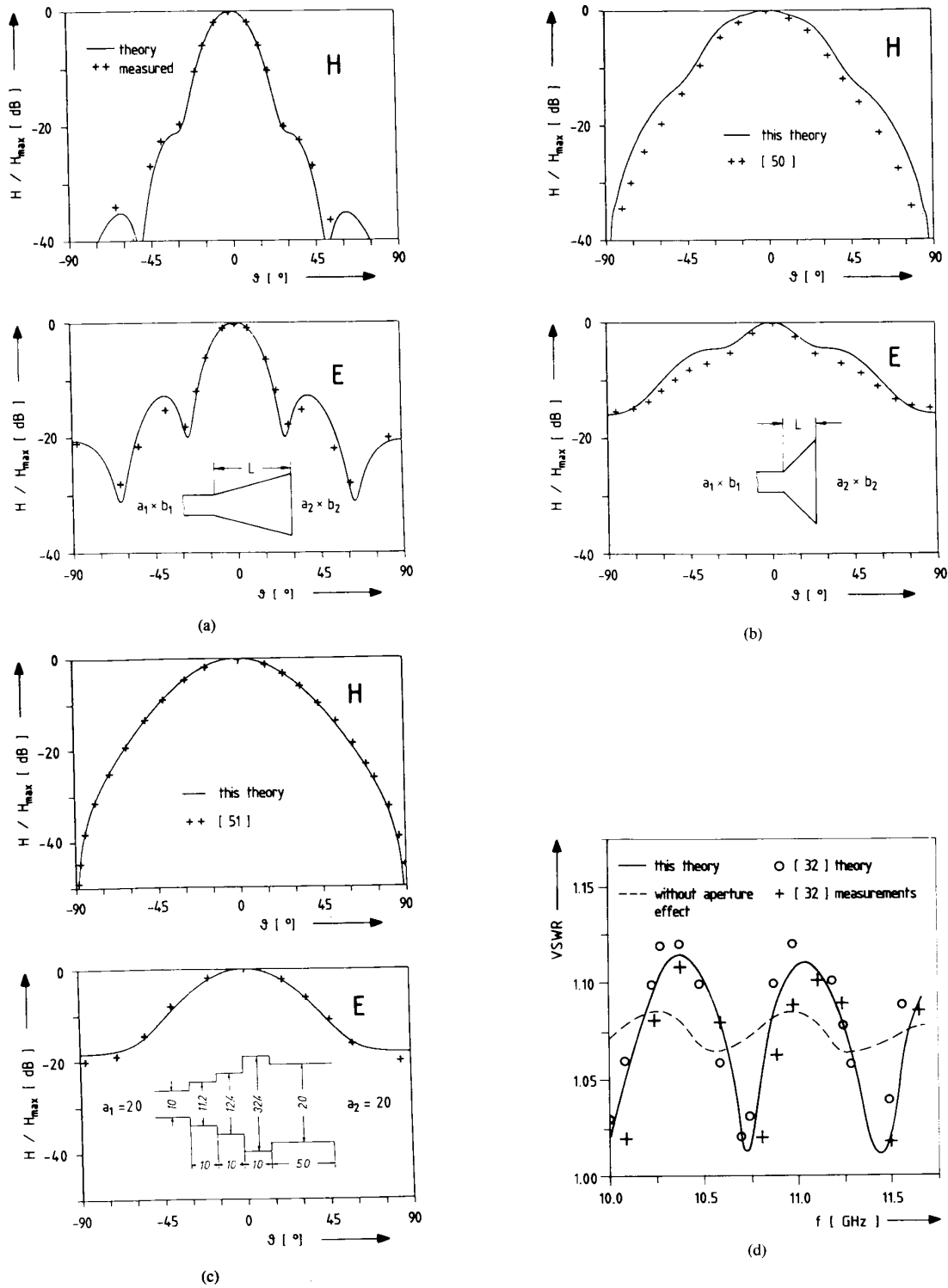


Fig. 2. Horn transitions. (a) *H*- and *E*-plane relative field pattern of a pyramidal "standard-gain" horn. $a_1 \times b_1 = 19.05 \text{ mm} \times 9.53 \text{ mm}$, $a_2 \times b_2 = 94.55 \text{ mm} \times 67.4 \text{ mm}$, $L = 202 \text{ mm}$. Frequency $f = 10 \text{ GHz}$ (+ + + measurements). (b) *H*- and *E*-plane relative field pattern of a pyramidal horn with large flare angle. $a_1 \times b_1 = 22.86 \text{ mm} \times 10.16 \text{ mm}$, $a_2 \times b_2 = 90 \text{ mm} \times 60 \text{ mm}$, $L = 30 \text{ mm}$. Frequency $f = 10 \text{ GHz}$ (+ + theory of [50]). (c) *H*- and *E*-plane pattern of a *E*-plane sector horn. $a_1 \times b_1 = 20 \text{ mm} \times 10 \text{ mm}$, $a_2 \times b_2 = 20 \text{ mm} \times 20 \text{ mm}$. Frequency $f = 20 \text{ GHz}$ (+ + theory of [51]). (d) Reflection coefficient at the throat of a pyramidal horn $a_1 \times b_1 = 22.86 \text{ mm} \times 10.16 \text{ mm}$, $a_2 \times b_2 = 84.7 \text{ mm} \times 72 \text{ mm}$, $L = 192 \text{ mm}$ (— this theory; - - - without aperture effect; ○○○ [32] theory; + + + [32] measurements).

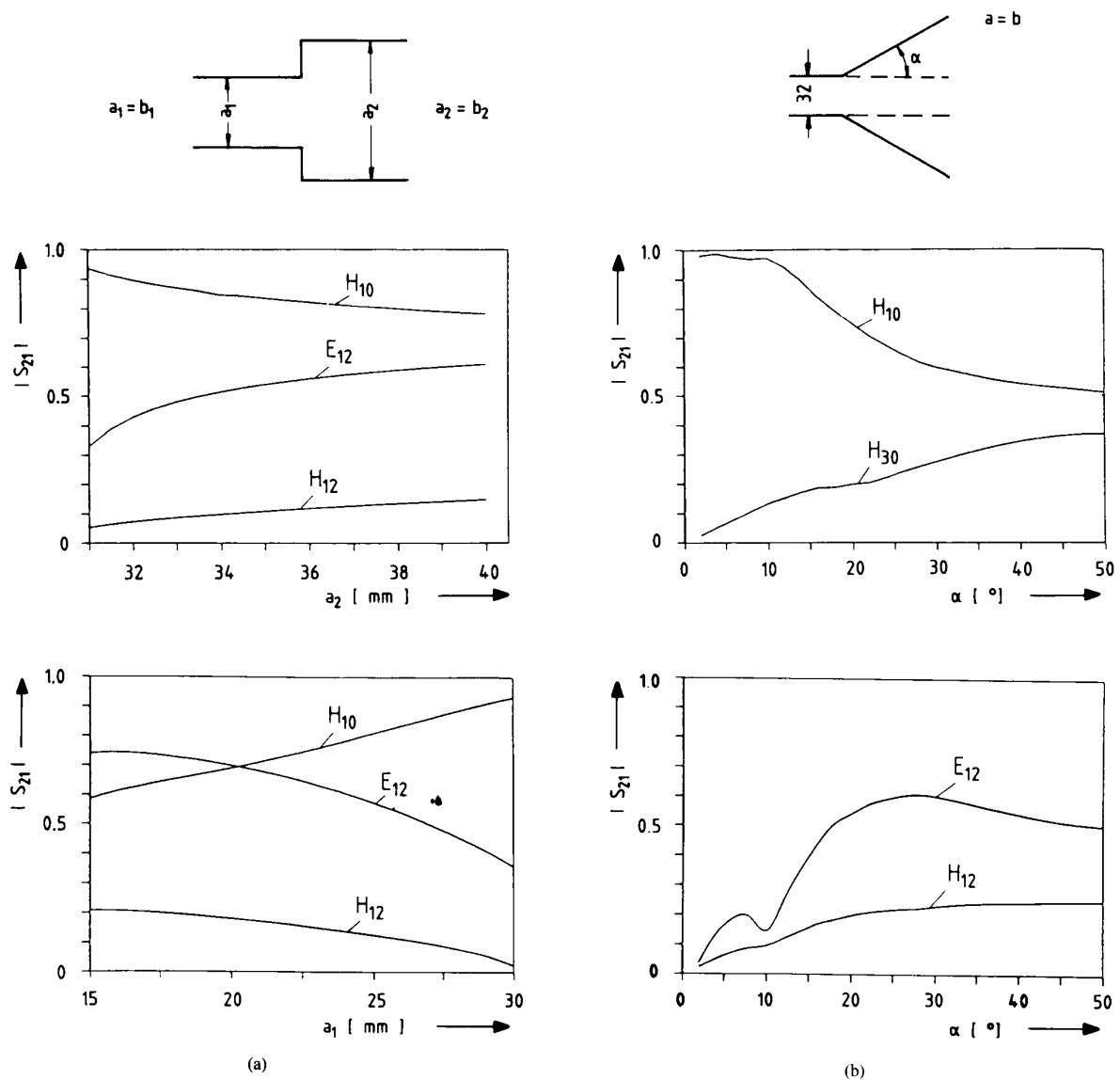


Fig. 3. Generation of modes by simple mode converters. (a) Double-plane step. $a_1 = b_1 = 25$ mm, and $a_2 = b_2 = 37$ mm, respectively, $f = 11$ GHz. (b) Horn transition with abruptly changing flare angle $f = 11$ GHz.

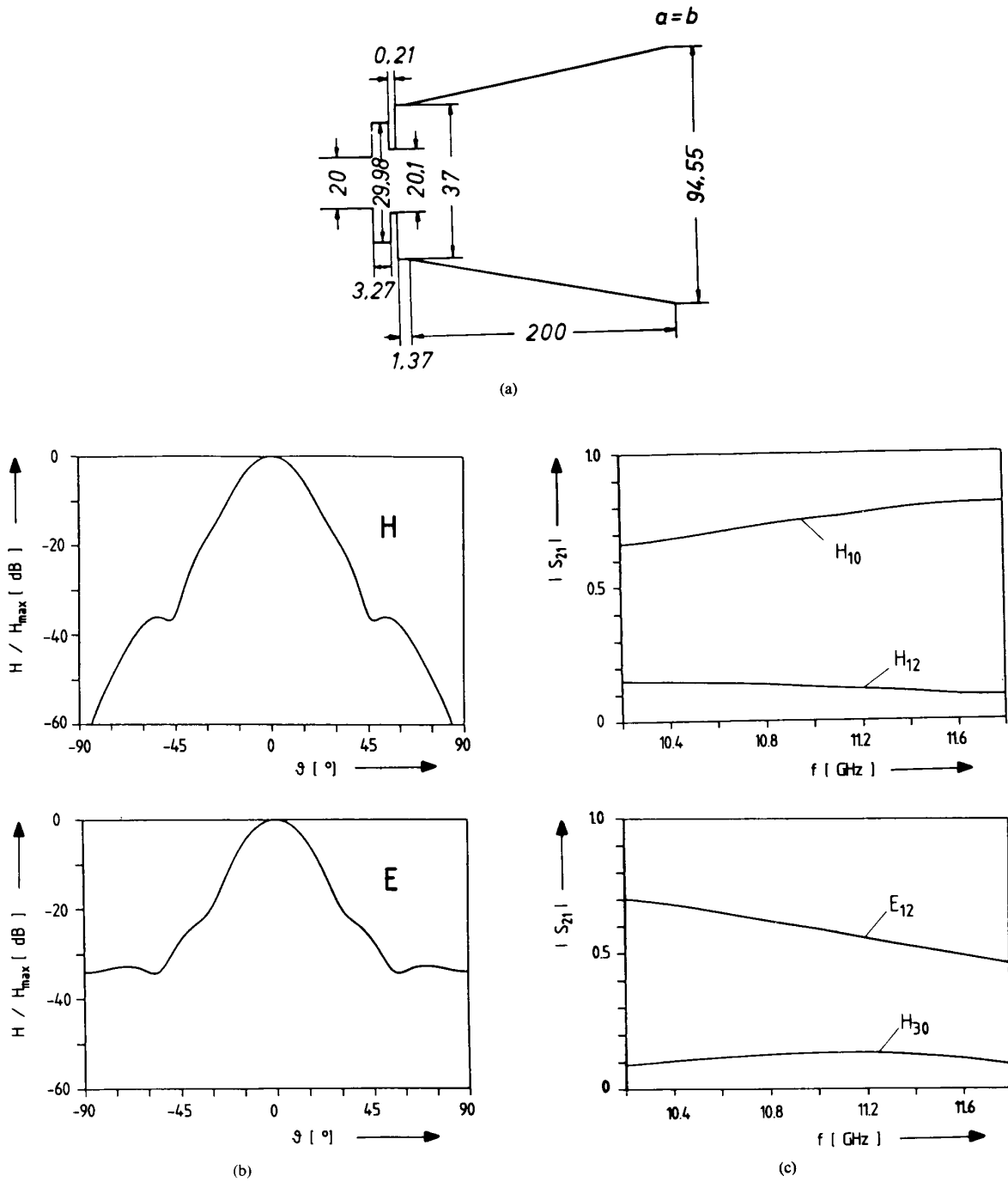


Fig. 4. Stepped multimode horn transition computer-optimized with regard to pattern symmetry. (a) Configuration (all dimensions in mm). (b) Relative field H - and E -plane pattern $f = 11.2$ GHz. (c) Scattering parameters $|s_{21}|$ of the throat region as a function of frequency.

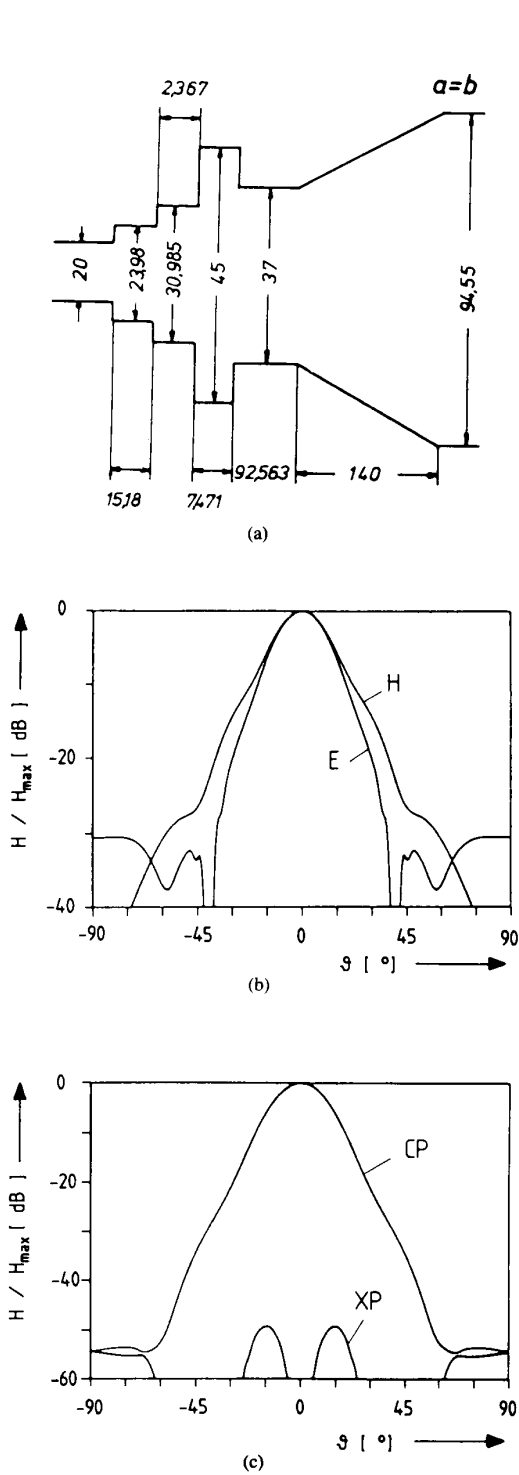


Fig. 5. Stepped multimode horn transition computer-optimized with regard to cross-polarization behavior. (a) Configuration (all dimensions in mm). (b) Relative field H - and E -plane pattern, $f = 11$ GHz. (c) Copolar and cross-polar pattern at $\phi = 45^\circ$, $f = 11$ GHz.

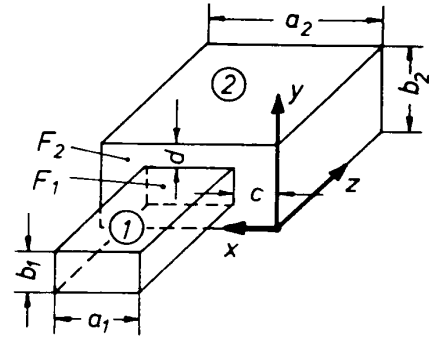


Fig. 6. Double-plane step module.

B. Normalized Eigenfunctions (3) of the Double-Plane Step Module (cf. Fig. 6)

$$T_{ekl}^{(i)} = \frac{2 \sin(k_x^{(i)}(x-c)) \sin(k_y^{(i)}(y-d))}{\sqrt{a_1 b_1 k_c^{(i)}}}$$

$$T_{hkl}^{(i)} = \frac{2 \cos(k_x^{(i)}(x-c)) \cos(k_y^{(i)}(y-d))}{\sqrt{a_1 b_1 k_c^{(i)} \sqrt{1 + \delta_{0k}} \sqrt{1 + \delta_{0l}}}}$$

$$T_{eij}^{(i+1)} = \frac{2 \sin(k_x^{(i+1)}x) \sin(k_y^{(i+1)}y)}{\sqrt{a_2 b_2 k_c^{(i+1)}}}$$

$$T_{hij}^{(i+1)} = \frac{2 \cos(k_x^{(i+1)}x) \cos(k_y^{(i+1)}y)}{\sqrt{a_2 b_2 k_c^{(i+1)} \sqrt{1 + \delta_{0i}} \sqrt{1 + \delta_{0j}}}} \quad (18)$$

with

$$k_c^{(s)} = \sqrt{k_x^{(s)2} + k_y^{(s)2}}$$

$$k_x^{(i)} = \frac{k\pi}{a_1} \quad k_y^{(i)} = \frac{l\pi}{b_1}$$

$$k_x^{(i+1)} = \frac{i\pi}{a_2} \quad k_y^{(i+1)} = \frac{j\pi}{b_2}$$

δ Kronecker-Delta.

C. Abbreviations in (8)

Indices:

$$pq_x = p_x + (q_x - 1)(L_x - 1);$$

$$p_x = 1, 2, \dots, (L_x - 1); \quad q_x = 1, 2, \dots, L_x;$$

$$pq_y = p_y + (q_y - 1)L_x;$$

$$p_y = 1, 2, \dots, L_x; \quad q_y = 1, 2, \dots, (L_y - 1);$$

L_x, L_y = total number of segments

in the x - and y -directions, respectively. (19)

Triangular functions:

$$T_w^u = \begin{cases} \frac{u - (w-1)\Delta u}{\Delta u}, & \text{for } (w-1)\Delta u \leq u \leq w\Delta u \\ \frac{-u + (w+1)\Delta u}{\Delta u}, & \text{for } w\Delta u \leq u \leq (w+1)\Delta u \\ 0 & \text{elsewhere;} \end{cases} \quad (20a)$$

with $u = x, y$; $w = p_u, q_u$, respectively.

Pulse functions:

$$P_w^v = \begin{cases} 1, & \text{for } (w-1)\Delta v \leq v \leq w\Delta v \\ 0, & \text{elsewhere} \end{cases} \quad (20b)$$

with $v = y, x$; $w = p_u, q_u$; $u = x, y$, respectively.

For simplicity, the relations in (20b) are given relative to a reference point (0, 0) in the lower left corner cf. Fig. 1(d).

D. Abbreviations in (10), (11), (12)

$$\vec{H}_{\tan}(\vec{M}_t) = \sum_{k=0}^M \sum_{l=0}^N (-j\sqrt{Y_{hkl}^*}) A_{thkl}^{wg} \vec{h}_{hkl} + \sum_{k=1}^M \sum_{l=1}^N (j\sqrt{Y_{ekl}}) A_{tekl}^{wg} \vec{h}_{ekl} \quad (21)$$

$$A_{thkl}^{wg} = j\sqrt{Y_{hkl}^*} \cdot \iint_{\text{aperture}} \vec{M}_t \cdot \vec{n} \times \vec{e}_{hkl} \cdot da \quad (22a)$$

$$A_{tekl}^{wg} = -j\sqrt{Y_{ekl}} \cdot \iint_{\text{aperture}} \vec{M}_t \cdot \vec{n} \times \vec{e}_{ekl} \cdot da \quad (22b)$$

$$B_{shkl}^{wg} = j\sqrt{Y_{hkl}^*} \cdot \iint_{\text{aperture}} \vec{W}_s \cdot \vec{h}_{hkl} \cdot da \quad (23a)$$

$$B_{sekl}^{wg} = -j\sqrt{Y_{ekl}} \cdot \iint_{\text{aperture}} \vec{W}_s \cdot \vec{h}_{ekl} \cdot da \quad (23b)$$

where the normalized wave amplitude coefficients $\vec{e}_e, \vec{e}_h, \vec{h}_e, \vec{h}_h$, due to all TE and TM modes in the waveguide, are given by the following expressions utilizing the normalized eigenfunctions \mathbf{T} , cf. (3) and (18),

$$\vec{e}_{e(r)} = \nabla(T_{e(r)}), \quad \vec{e}_{h(r)} = \vec{n} \times \nabla(T_{h(r)}) \quad (24a)$$

$$\vec{h}_{e(r)} = \vec{n} \times \nabla(T_{e(r)}), \quad \vec{h}_{h(r)} = \nabla(T_{h(r)}). \quad (24b)$$

r replaces the indices kl , or ij , respectively, and \vec{n} is the unit vector in z -direction (i.e., normal to the aperture). Y are the wave admittances of the TE and TM waves under consideration

$$Y_{h(r)} = \gamma_{h(r)} / (j\omega\mu), \quad Y_{e(r)} = (j\omega\mu) / \gamma_{e(r)}, \quad (25)$$

and γ is a propagation factor in its usual formulation for propagating waves and evanescent fields using the corres-

ponding cut-off wavenumber k_c

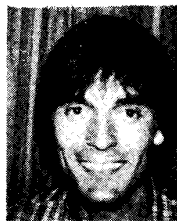
$$\gamma = \sqrt{\omega_{\mu\epsilon}^2 - k_c^2}. \quad (26)$$

The asterisk in (22), (23) denotes the conjugate complex wave admittances due to the normalization to the complex power. The application of Galerkin's method [7] requires an inner product (22), (23) with normalized weighting functions \vec{W} that are equal to the normalized basis functions (7).

REFERENCES

- [1] N. Marcuvitz, *Waveguide Handbook*. New York: McGraw-Hill, 1951, pp. 179-216.
- [2] R. E. Collin, *Field Theory of Guided Waves*. New York: McGraw-Hill, 1960, ch. 7.3.
- [3] R. F. Harrington, *Time-Harmonic Electromagnetic Fields*. New York: McGraw-Hill, 1961, ch. 3.
- [4] W. F. Crosswell, R. C. Rudduck, and D. M. Hatcher, "The admittance of a rectangular waveguide radiating into a dielectric slab," *IEEE Trans. Antennas Propagat.*, vol. AP-15, pp. 627-633, Sept. 1967.
- [5] R. F. Harrington, *Field Computation by Moment Methods*. New York: MacMillan, 1968, ch. 1, 5.
- [6] H. Y. Yee and L. B. Felson, "Ray-optical analysis of electromagnetic scattering in waveguide," *IEEE Trans. Microwave Theory Tech.*, vol. MTT-17, pp. 671-683, Sept. 1969.
- [7] R. F. Harrington and J. R. Mautz, "A generalized network formulation for aperture problems," *IEEE Trans. Antennas Propagat.*, vol. AP-24, pp. 870-873, Nov. 1976.
- [8] —, "Electromagnetic transmission through an aperture in a conducting plane," *AEU*, vol. 31, pp. 81-87, Feb. 1977.
- [9] A. R. Jamieson and T. E. Rozzi, "Rigorous analysis of cross-polarization in flange-mounted rectangular waveguide radiators," *Electron. Lett.*, vol. 13, pp. 742-744, Nov. 1977.
- [10] J. R. Mautz and R. F. Harrington, "Transmission from a rectangular waveguide into half space through a rectangular aperture," *IEEE Trans. Microwave Theory Tech.*, vol. MTT-26, pp. 44-45, Jan. 1978.
- [11] R. H. McPhie and A. I. Zaghoul, "Radiation from a rectangular waveguide with infinite flange—Exact solution by the correlations matrix method," *IEEE Trans. Antennas Propagat.*, vol. AP-28, pp. 497-503, July 1980.
- [12] V. Teodoridis, T. Spicopoulos, and F. E. Gardiol, "The reflection from an open-ended rectangular waveguide terminated by a layered dielectric medium," *IEEE Trans. Microwave Theory Tech.*, vol. MTT-33, pp. 359-366, May 1985.
- [13] J. A. Encinar and J. M. Rebolgar, "Convergence of numerical solutions of open-ended waveguide by modal analysis and hybrid modal-spectral techniques," *IEEE Trans. Microwave Theory Tech.*, vol. MTT-34, pp. 809-814, July 1986.
- [14] P. D. Potter, "A new horn antenna with suppressed sidelobes and equal beamwidth," *Microwave J.*, vol. 6, pp. 71-78, June 1963.
- [15] H. M. Pickett, J. C. Hardy, and J. Farhoomand, "Characterisation of a dual-mode horn for submillimeter wavelengths," *IEEE Trans. Microwave Theory Tech.*, vol. MTT-32, pp. 936-937, Aug. 1984.
- [16] E. Lier, "Cross polarization from dual mode horn antennas," *IEEE Trans. Antennas Propagat.*, vol. AP-34, pp. 106-110, Jan. 1986.
- [17] P. J. B. Clarricoats and P. K. Saha, "Propagation and radiation behavior of corrugated feeds," *Proc. Inst. Elec. Eng.*, vol. 118, no. 9, pp. 1167-1186, Sept. 1971.
- [18] A. W. Rudge, K. Milne, A. D. Olver, and P. Knight, *The Handbook of Antenna Design*. London, U.K.: Peregrinus, 1982, vol. 1, ch. 4.6.
- [19] P. J. B. Clarricoats and A. D. Olver, *Corrugated Horns for Microwave Antennas*. London, U.K.: Peregrinus, 1983, ch. 3.7.
- [20] G. H. Bryant, "Propagation in corrugated waveguides," *Proc. Inst. Elec. Eng.*, vol. 116, pp. 203-213, Feb. 1969.
- [21] R. Baldwin and P. McInnes, "A rectangular corrugated feed horn," *IEEE Trans. Antennas Propagat.*, vol. AP-23, pp. 314-317, Nov. 1975.
- [22] G. L. James, "Analysis and design of TE₁₁-to-HE₁₁ corrugated cylindrical waveguide mode converters," *IEEE Trans. Microwave Theory Tech.*, vol. MTT-29, pp. 1059-1066, Oct. 1981.
- [23] V. Hombach and H. Severin, "Berechnung der Kreuzpolarization im Fernfeld von Hohlleitungstrahlern," *AEU*, vol. 37, pp. 101-107, Mar./Apr. 1983.

- [24] E. Kühn and V. Hombach, "Computer-aided analysis of corrugated horns with axial or ring-loaded radial slots," in *Proc. ICAP-83*, pp. 127-131.
- [25] D. Fasold and H. Pecher, "Gain of rectangular corrugated horns," *Microwave J.*, vol. 22, pp. 124-128, Mar. 1979.
- [26] C. C. Han and A. N. Wickert, "A new rectangular horn antenna generating a circularly polarized elliptical beam," *IEEE Trans. Antennas Propagat.*, vol. AP-22, pp. 746-751, Nov. 1974.
- [27] R. C. Menezes and S.-W. Lee, "Analysis of rectangular horn antennas via uniform asymptotic theory," *IEEE Trans. Antennas Propagat.*, vol. AP-30, pp. 241-250, Mar. 1982.
- [28] E. Kühn and B. K. Watson, "Rectangular corrugated horns—Analysis, design, and evaluation," in *Proc. 14th European Microwave Conf.*, Sept. 1984, pp. 221-227.
- [29] L. Botha and D. A. McNamara, "Examination of antenna patterns of profiled horns using the method of moments," in *IEEE Antennas Propagat. Soc. Int. Symp. Dig.*, Vancouver, June 1985, pp. 293-296.
- [30] E. Kühn and B. Watson, "Computer-aided design and performance evaluation of fully corrugated rectangular horns," in *IEEE Antennas Propagat. Soc. Int. Symp. Dig.*, Philadelphia, June 1986, pp. 795-798.
- [31] C. Dragone, "A rectangular horn of four corrugated plates," *IEEE Trans. Antennas Propagat.*, vol. AP-33, pp. 160-164, Feb. 1985.
- [32] J. A. Encinar and J. M. Rebolgar, "Hybrid technique for analyzing corrugated and noncorrugated rectangular horns," *IEEE Trans. Antennas Propagat.*, vol. AP-34, pp. 961-968, Aug. 1986.
- [33] Y. Nikawa, T. Katsumata, M. Kikuchi, and S. Mori, "An electric field converging applicator with heating pattern controller for microwave hyperthermia," *IEEE Trans. Microwave Theory Tech.*, vol. MTT-34, pp. 631-635, May 1986.
- [34] J. R. Wait, "Analysis of the radiation leakage for a four-aperture phased-array applicator in hyperthermia therapy," *IEEE Trans. Microwave Theory Tech.*, vol. MTT-34, pp. 539-541, May 1986.
- [35] H. Patzelt, and F. Arndt, "Double-plane steps in rectangular waveguides and their application for transformers, irises, and filters," *IEEE Trans. Microwave Theory Tech.*, vol. MTT-30, pp. 771-776, May 1982.
- [36] U. Tucholke, F. Arndt, and T. Wriedt, "Field theory design of square waveguide irises polarizers," *IEEE Trans. Microwave Theory Tech.*, vol. MTT-34, pp. 156-160, Jan. 1986.
- [37] F. Arndt, B. Koch, J. Orlok and N. Schröder, "Field theory design of rectangular waveguide broad-wall metal-insert slot couplers for millimeter-wave applications," *IEEE Trans. Microwave Theory Tech.*, vol. MTT-33, pp. 95-104, Feb. 1985.
- [38] H. Schmiedel and F. Arndt, "Mode transducer utilizing asymmetric waveguide narrow-wall coupling," in *Proc. 15th European Microwave Conf.*, Paris, Sept. 1985, pp. 737-742.
- [39] K. R. Goudey and A. F. Sciambi, "High power X-band monopulse tracking feed for the Lincoln laboratory long-range imaging radar," *IEEE Trans. Microwave Theory Tech.*, vol. MTT-26, pp. 326-332, May 1978.
- [40] M. S. Navarro, T. E. Rozzi, and Y. T. Lo, "Propagation in a rectangular waveguide periodically loaded with resonant irises," *IEEE Trans. Microwave Theory Tech.*, vol. MTT-28, pp. 857-867, Aug. 1980.
- [41] W. L. Ko, V. Jamnejad, R. Mittra, and S.-W. Lee, "Radiation from an open-ended waveguide with beam equalizer—A spectral domain analysis," *IEEE Trans. Antennas Propagat.*, vol. AP-30, pp. 44-53, Jan. 1982.
- [42] H. Schmiedel, "Anwendung der Evolutionsoptimierung bei Mikrowellenschaltungen," *Frequenz*, vol. 35, pp. 306-310, Nov. 1980.
- [43] F. Arndt, U. Tucholke, and T. Wriedt, "Computer-optimized multi-section transformers between rectangular waveguides of adjacent frequency bands," *IEEE Trans. Microwave Theory Tech.*, vol. MTT-32, pp. 1479-1484, Nov. 1984.
- [44] A. J. Fenn, G. A. Thiele, and B. A. Munk, "Moment method analysis of finite rectangular waveguide phased arrays," *IEEE Trans. Antennas Propagat.*, vol. AP-30, pp. 554-563, July 1982.
- [45] R. F. Harrington and J. R. Mautz, "A generalized network formulation for aperture problems," Syracuse, NY, Sci. Rep. 8, Contract F19628-73-C-0047, A. F. Cambridge Res. Lab. and Syracuse Univ., Nov. 1975.
- [46] J. R. Mautz and R. F. Harrington, "Electromagnetic transmission through a rectangular aperture in a perfectly conducting plane," A. F. Cambridge Res. Lab. and Syracuse Univ., Syracuse, NY, Sci. Rep. 10, Contract F19628-73-C-0047, Feb. 1976.
- [47] J. R. Mautz and R. F. Harrington, "Transmission from a rectangular waveguide into half space through a rectangular aperture," A. F. Cambridge Res. Lab. and Syracuse Univ., Syracuse, NY, Sci. Rep. 12, Contract F19628-73-C-0047, Aug. 1976.
- [48] H. Auda and R. F. Harrington, "A moment solution for waveguide junction problems," *IEEE Trans. Microwave Theory Tech.*, vol. MTT-31, pp. 515-519, July 1983.
- [49] J. A. Encinar and J. M. Rebolgar, "Accurate analysis of feed-horns by a hybrid modal-spectral method," in *IEEE Antennas Propagat. Soc. Int. Symp. Dig.*, Vancouver, June 1985, pp. 331-334.
- [50] ———, "Radiation from open ended waveguide by hybrid modal-spectral method," in *Proc. MELECON'85*, vol. 3, 1985, pp. 201-205.
- [51] J. M. Jarem, "The input impedance and antenna characteristics of a cavity-backed plasma covered ground plane antenna," *IEEE Trans. Antennas Propagat.*, vol. AP-34, pp. 262-267, Feb. 1986.



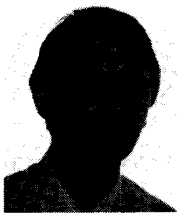
Thomas Wriedt was born in Preetz, West Germany, on June 20, 1954. He received the Ing. grad. degree from the Fachhochschule Kiel in 1979, and the Dipl. Ing. and the Dr. Ing. degrees from the University of Bremen in 1983 and 1986, respectively.

From 1984 to 1986 he worked as a Research Assistant, designing microwave components and antennas at the University of Bremen. He is currently working on signal analysis in laser Doppler anemometry with the Mechanical Processing

Department at the same university.

Fritz Arndt (SM'83), for a photograph and biography please see page 338 of the March 1989 issue of this TRANSACTIONS.

Karl-Heinz Wolff, for a photograph and biography please see page 338 of the March 1989 issue of this TRANSACTIONS.



Ulrich Tucholke was born in Klein-Sehlingen, West Germany, on June 20, 1956. He received the Dipl.-Ing. (FH) from the Hochschule für Technik Bremen, Germany, in 1979, and the Dipl.-Ing. and Dr.-Ing. degrees from the University of Bremen, Germany, in 1983 and 1987, respectively.

From 1983 to 1987, Dr. Tucholke worked as a Scientific Assistant with Professor Arndt at the Microwave Department of the University of Bremen, concentrating on passive millimeter-wave components, such as iris-coupled waveguide filters and polarizers. Since 1988, he has been with the Bremer Institut für Betriebstechnik und angewandte Arbeitswissenschaften (BIBA), where he performs research on computer-aided design technologies, focusing on neutral interfaces between different graphic systems.